Extraordinary refraction and dispersion in two-dimensional photonic-crystal slabs

Wounjhang Park

Department of Electrical and Computer Engineering, University of Colorado, Boulder, Colorado 80309-0425

Christopher J. Summers

Phosphor Technology Center of Excellence, School of Materials Science and Engineering, Georgia Institute of Technology, Atlanta, Georgia 30332-0245

Received March 28, 2002

Studies of the refraction and dispersion properties of two-dimensional (2D) photonic-crystal (PC) slab waveguides are reported. The photonic band structure is strongly modified in a slab PC, and only a small number of bands satisfy the guiding conditions imposed by the lack of translation symmetry in the direction perpendicular to the slab; however, it was found that a significant number of the guided modes retain the giant refraction and strong dispersion properties discovered previously in pure 2D PCs. A small change in incident angle resulted in a dramatic change in refraction angle. Furthermore, the dispersion surface exhibited a strong dependence on the frequency, resulting in a superprism effect similar to what has been predicted for pure 2D PCs. In the silicon-based slab PC studied, refraction angles as high as nearly 70° were predicted for incident angles of less than 7°, and frequency components differing by 3% were separated by 15°. The demonstration of giant refraction and superprism phenomena in slab waveguide PCs open the possibility of developing new classes of optical devices that can, for example, be used to develop 2D optical integrated circuits for communications and computing.

OCIS codes: 230.7400, 130.3120.

During the past ten years or so a new class of materials, photonic crystals (PCs), have been extensively studied for their unique optical properties and for the novel devices that they may engender.[1,2] Among the many unconventional optical properties of PCs are their giant refraction and strong dispersion characteristics, which may become orders of magnitude greater than in conventional optical materials. These novel phenomena were first reported by Lin *et al.* in the millimeter-wave region.[3] Kosaka *et al.* then discovered similar phenomena at optical wavelengths in a complex three-dimensional (3D) structure of $Si-SiO_2$.[4] They were later predicted to be possible as well in far-simpler two-dimensional (2D) systems.[5] These novel properties present an exciting possibility for achieving microphotonic and nanophotonic devices that can collect, focus, disperse, switch, and steer light. It should be noted that these properties are based on anisotropic and nonlinear dispersion and therefore do not require the existence of photonic bandgaps, thus significantly relieving material requirements.

Although there have been some successful demonstrations of giant refraction and superprism effects, the fabrication of PCs remains a challenge because it requires either a complicated self-replicating deposition technique for 3D PCs or a means of creating extremely long structures to simulate pure 2D PCs. In this respect 2D PC slabs with finite thickness represent more-realistic structures that can be fabricated by the conventional thin-film deposition and lithography techniques commonly used in the electronics industry. Consequently, 2D slab PCs have been the subject of extensive research in recent years.[6–8] A slab PC typically consists of a thin layer of high-index material, which is periodically patterned. The slab may lie on a low-index substrate or be suspended in air. In either case the electromagnetic field is scattered by the periodic structure in the plane of the dielectric slab and at the same time is confined within the slab as a consequence of the index profile in the direction perpendicular to the slab. Therefore the confinement of light within the slab is imperfect, and only modes that satisfy the total-internal-reflection condition survive; the rest radiate into the surrounding media with short lifetimes. This imperfect light confinement consequently imposes limitations on the functionality of slab PCs. However, it was reported recently that not all radiation modes are short lived and that certain modes actually have extremely long lifetimes despite the fact that they do not satisfy the guiding conditions.[9,10] These results have foreshadowed the possibility of overcoming the limitations of slab PCs and realizing novel device structures that are compatible with existing fabrication techniques. In this paper we report the refraction and dispersion properties of 2D slab PCs and show that the novel properties that have been predicted for 2D and 3D PCs are also realizable in slab PCs.

The system studied here is a thin slab of silicon (Si) ($\epsilon = 12$) patterned with a triangular array of air ($\epsilon = 1$) holes. The optical properties of the Si slab PCs were investigated for various air-hole diameters and slab thicknesses. The theoretical studies were carried out with the FDTD method.[11,12] The unit cell of the 2D triangular PC was discretized into 16×16 grid points. The number of grid points in the vertical direction was set to yield the same spatial resolution and was changed according to the slab thickness. The computation cell consisted of three layers: a dielectric slab with an air hole, an air layer, and an absorbing boundary layer. Only the upper half of the

0146-9592/02/161397-03$15.00/0

dielectric slab was defined with a mirror boundary condition imposed at the computation cell boundary. This system simulates a symmetric slab surrounded by air on both sides, in which case all modes are either even or odd under the reflection in the symmetry plane. By imposing the mirror boundary condition, we reduced the computation load by half, and it is also possible to select even or odd modes. In the plane of the slab we used the periodic boundary condition according to Bloch's theorem. The thickness of the air layer was varied between $2a$ and $4a$ where a is the lattice constant, that is, the distance between two adjacent air holes. The absorbing boundary layer was used to prevent unphysical reflections from the computation cell boundary and to simulate infinitely large air layers. For this purpose we used the Berenger-type perfectly matched layer boundary condition.[13] More specifically, we used an implementation of perfectly matched layer similar to that originally developed by Zhao and Cangellaris[14] but modified to work properly with the nonorthogonal coordinate system used for the triangular periodicity in the slab.

Figure 1 shows the photonic band structure calculated by the FDTD method for a Si waveguide patterned with a triangular array of air holes. The photon energy is plotted in terms of the normalized frequency, $\omega a/2\pi c$. The air-hole diameter was $0.4a$, and the slab thickness was $0.5a$. In this figure, only the even modes are displayed. The light cone is the boundary between the shaded and the unshaded regions. Modes in the shaded region are therefore unbounded (radiation) modes, and those lying below the light line are confined within the slab. The imposition of the guiding condition through the light cone is the key difference between the band structures of a 2D slab PC and a pure 2D PC. For a slab PC, as seen in Fig. 1, there is no true photonic bandgap, because of the continuum of radiation modes outside the light cone. Instead, one can define a new bandgap in which there is no guided mode. Figure 1 shows that this particular Si slab PC has two bandgaps between normalized frequencies of 0.25–0.27 and 0.37–0.39 for the even modes. Despite the drastic change in band structure, the slab PC proved to exhibit anisotropic dispersion surfaces similar to what was found in a pure 2D PC.[5] The inset of Fig. 2 shows the dispersion diagram calculated at a normalized frequency of 0.357. The circle is the cross section of the light cone inside which no guided modes may exist. Although the diagram is partially cut away by the light cone, a significant portion of the dispersion diagram, which is highly anisotropic and exhibits sharp inflection points along the Γ–M directions, still lies within the guiding regime. Since the group velocity is defined by the gradient of the dispersion surface, the light-propagation direction may be predicted from the shape of the dispersion diagram. Using the method outlined previously,[5] we calculated the refraction angle as a function of incident angle. As shown in Fig. 2, at a normalized frequency of 0.357 the refraction angle changed from 0° to more than 70° as the incident angle, measured in reference to the Γ–M direction, was varied from 0° to 7°. It should be pointed out that the cutoff is reached at an incident angle of 11° as indicated in Fig. 2, and thus the entire variation of 70° in the refraction angle was achieved within the guiding regime. The giant refraction properties were also strongly frequency dependent, leading to an extraordinary dispersion (superprism) effect. As shown in Fig. 2, for a range of normalized frequencies between 0.357 and 0.364, the refraction angle rapidly decreases as the frequency is increased. For a fixed incident angle of 2°, the refraction angle increased from 35° to 56° as the frequency was decreased from 0.364 to 0.357, yielding more than 21° separation in the refraction angle for a 2% change in frequency. This corresponds to ~8 nm in the visible spectrum and to ~0.03 μm near the communication wavelength of 1.54 μm. This strong dispersion effect is due to the rapid contraction of the dispersion curve with increasing frequency. This process unfortunately moves a greater portion of the dispersion diagram inside the cutoff circle where it becomes radiation modes. Therefore, as indicated in Fig. 2, the cutoff occurs at a smaller incident angle for a higher normalized frequency, thus limiting the range of refraction angles attainable with guided modes.

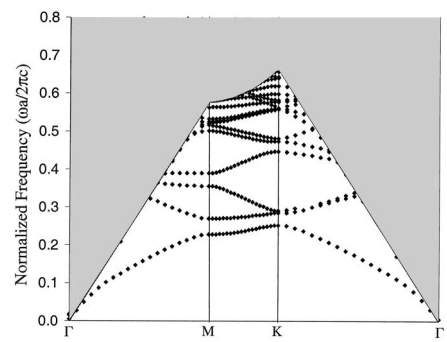

Fig. 1. Photonic band structure of a thin slab of Si patterned with a 2D triangular lattice of air holes. Only the even modes with respect to reflection in the mirror plane are displayed.

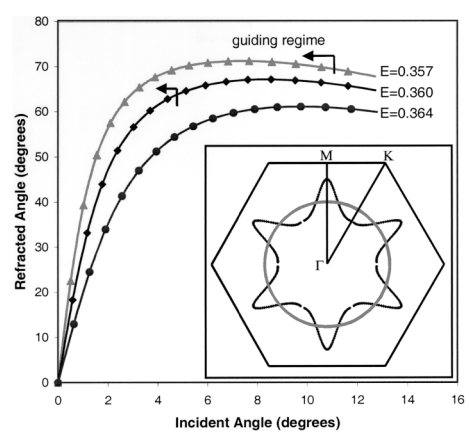

Fig. 2. Calculated refraction angles for normalized frequencies between 0.357 and 0.364. The incident angle is measured from the Γ–M direction. Inset, dispersion diagram calculated at a normalized frequency of 0.357. The circle represents the cutoff line outside of which is the guiding regime.

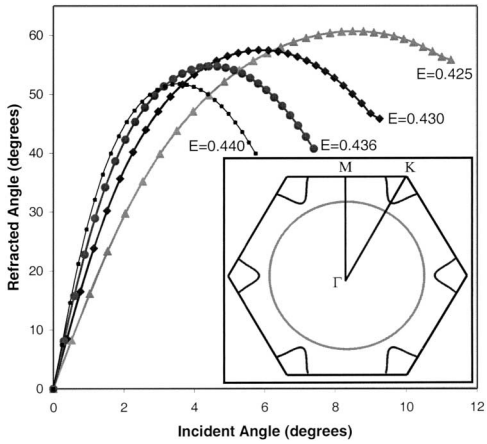

Fig. 3. Calculated refraction angles for normalized frequencies between 0.425 and 0.440. The incident angle is measured from the Γ−K direction . Inset, dispersion diagram calculated at a normalized frequency of 0.430. The circle represents the cutoff line outside of which is the guiding regime.

This problem, however, is not intrinsic to the structure. At a different frequency range we found that the same structure exhibits a similar giant refraction and superprism effect entirely within the guiding regime. The inset of Fig. 3 shows the dispersion diagram calculated for a normalized frequency of 0.430. As shown, the dispersion diagram is anisotropic and shows a sharp negative curvature along the Γ−K direction. This leads to giant negative refraction, in which the light is bounced back to the same side in which it was incident. Figure 3 shows the calculated refraction angle as a function of incident angle, which is now measured with respect to the Γ−K direction. At a normalized frequency of 0.430, for example, the refraction angles were found to change from 0° to nearly 60° as the incident angle was varied from 0° to 6°. This giant negative refraction effect also exhibited a strong frequency dependence, as shown in Fig. 3. At small incident angles, the refraction angle increased with increasing frequency, opposite to what was observed in Fig. 2. For an incident angle of 2°, the refraction angle was increased from 29° to 44° as the normalized frequency was increased from 0.425 to 0.440, yielding a 15° separation for a 3% change in frequency. This phenomenon has an origin similar to the case of Fig. 2; that is, the dispersion curve shifts rapidly as the frequency is changed. However, it should be emphasized that in this case the entire dispersion curve lies outside the cutoff circle at all frequencies, and thus the observed giant refraction and superprism effects are achieved with guided modes only.

In summary, we have presented a study of the refraction and dispersion properties of slab PCs. The photonic band structure is significantly modified because of the lack of translation symmetry in the direction perpendicular to the slab. Only a small number of the photonic bands are confined and guided within the slab, whereas the remainder lie outside the light cone and radiate out of the slab. Despite such modifications to the band structure, the slab PC retains the giant refraction and high-dispersion properties discovered previously in pure 2D PCs in which infinitely long structures were assumed. Our FDTD simulations predicted a highly anisotropic dispersion surface within the guiding regime. A small change in incident angle resulted in a dramatic change in refraction angle. Furthermore, the dispersion surface exhibited a strong dependence on the frequency, resulting in the superprism effect similar to what has been predicted for pure 2D PCs. The Si-based slab PC investigated in this paper exhibited refraction angles as great as 70° for incident angles less than 7°. Also, a 3% change in light frequency was predicted to cause as much as a 15° change in refraction angle. The demonstration of giant refraction and superprism phenomena within the guiding regime in a slab PC has great practical significance. Slab PCs are highly compatible with conventional semiconductor processing technologies, thus opening up new possibilities for designing and fabricating monolithically integrated optical devices for signal processing, communications, and computing.

The authors gratefully acknowledge S.-Y. Lin for helpful discussions and C. W. Neff for his support in the computations. Financial support from Defense Advanced Research Projects Agency (DARPA) grant MDA972-93-1-0030 and Army Research Office grant DAAD19-01-1-0603 are gratefully acknowledged. W. Park's e-mail address is wpark@colorado.edu.

References

1. E. Yablonovitch, Phys. Rev. Lett. **63,** 1950 (1987).
2. See, for example, J. D. Joannopoulos, R. D. Meade, and J. N. Winn, *Photonic Crystals: Molding the Flow of Light* (Princeton University, Princeton, N.J., 1995).
3. S.-Y. Lin, V. M. Hietala, L. Wang, and E. D. Jones, Opt. Lett. **21,** 1771 (1996).
4. H. Kosaka, T. Kawashima, A. Tomina, M. Notomi, T. Tamamura, T. Sato, and S. Kawakami, Phys. Rev. B **58,** 10096 (1998).
5. W. Park, J. S. King, C. W. Neff, C. Liddell, and C. J. Summers, Phys. Status Solidi B **229,** 949 (2002).
6. S. G. Johnson, S. Fan, P. R. Villeneuve, J. D. Joannopoulos, and L. A. Kolodziejski, Phys. Rev. B **60,** 5751 (1999).
7. O. Painter, K. Srinivasan, J. D. O'Brien, A. Scherer, and P. D. Dapkus, J. Opt. A **3,** S161 (2000).
8. H. Benisty, C. Weisbuch, D. Labilloy, M. Rattier, C. J. M. Smith, T. F. Krauss, R. M. De La Rue, R. Houdre, U. Oesterle, C. Jouanin, and D. Cassagne, J. Lightwave Technol. **17,** 2063 (1999).
9. T. Ochiai and K. Sakoda, Phys. Rev. B **63,** 125108 (2001).
10. P. Paddon and J. F. Young, Phys. Rev. B **61,** 2090 (2000).
11. C. T. Chan, Q. L. Lu, and K. M. Ho, Phys. Rev. B **51,** 16635 (1995).
12. A. J. Ward and J. B. Pendry, Comput. Phys. Commun. **112,** 23 (1998).
13. J. P. Berenger, J. Comput. Phys. **114,** 185 (1994).
14. L. Zhao and A. C. Cangellaris, IEEE Trans. Microwave Theory Tech. **44,** 2555 (1996).